

EXTENSION TO FAULT LOCATION ALGORITHM BASED ON SYNCHRONIZED SAMPLING

A. Gopalakrishnan, M. Kezunovic*
Texas A&M University (TAMU)
College Station, Texas, U.S.A

S. M. McKenna, D. M. Hamai
Western Area Power Administration
Golden, Colorado, U.S.A

Summary– The use of Global Positioning System (GPS) of satellites has allowed the synchronization of voltage and current measurements from a wide–area power system. Using raw samples of voltage and current from the two ends of a transmission line, algorithms for fault analysis and fault location have been developed at TAMU. In this paper, a brief review of those techniques is provided. The fault location algorithm that has been developed is capable of handling system conditions like changing fault resistance, mutual coupling and multi–terminal lines. The fault location algorithm is briefly explained, and some results from testing the algorithm on an EMTP model of a power system are provided. Some of the issues involved in implementing the algorithm in the field are also discussed.

Keywords– Fault Location, Fault Analysis, Synchronized Sampling, Electromagnetic Transients Program.

1. INTRODUCTION

In the past few years, a number of applications have been reported that use the Global Positioning System (GPS) of satellites to accurately acquire synchronous voltage and current information from a wide–area power system, [1,2]. Specialized data acquisition equipment is used to time–tag the data and convert them to a complex phasor quantity. These phasors are then used in a number of functions like state estimation, transient stability prediction, adaptive out–of–step relaying, model validation etc. Some of these functions have been implemented in the Wide–Area Measurement System (WAMS), by the Bonneville and Western Area Power Administrations, under the sponsorship of the US Department of Energy (DOE) and the Electric Power Research Institute (EPRI) [3]. An alternative to computing phasors from samples is to use the samples directly in the function for which the samples are intended for.

Such an approach has been adopted for the purposes of fault analysis [4,5,6,7], that includes the functions of fault detection, classification and location. These methods are very general in nature and can handle special conditions like changing fault resistance, mutual coupling and multi–terminal lines. They are not influenced by the fault incidence angle or the fault impedance. Data from both ends of the line is used; therefore no assumptions are made regarding the remote source impedance, the line geometry, line loading or other system conditions. The result is a set of techniques that are extremely robust, fast and accurate. It can therefore be said that a good fault analysis technique must perform well under the various conditions described above.

The voltage and current data are applied to a suitable model of the transmission line. The mathematical model relates the acquired data to the line parameters of resistance, inductance and capacitance. The quantity of interest, (e.g.: fault location) is then extracted from the resulting equations.

In this paper, we will review the fault analysis methods, concentrating on the fault location in a little detail. Some results from testing the fault location algorithm on a sample power system are provided to show that the algorithm does satisfy the required criteria.

The implementation of the algorithms in a field instrument introduces a number of salient points that are discussed after the presentation of the test results.

2. ALGORITHM REQUIREMENTS

A truly robust fault location algorithm must be highly accurate under a number of operating and fault conditions such as:

- Long and short transmission lines
- Parallel lines

* Department of Electrical Engineering, Texas A&M University, College Station, Texas 77843-3128

- Multi-terminal lines
- Transposed and untransposed lines
- High and low loading fault fed from both ends
- Faults with time-varying fault resistance
- Faults of any type and incidence angle

To satisfy the requirements detailed above, a fault location algorithm must acquire data from all ends of the transmission line. Existing algorithms compute phasors from the acquired samples of voltage and current. The need to estimate phasors introduces difficulty in high-speed tripping situations where the algorithm may not be able to determine the fault location accurately before the current signals disappear because of the relay operation and circuit breaker opening.

To get around this problem, samples of voltage and current can be used directly in the fault location algorithm. The samples are applied to a model of the transmission line in the time-domain and solved for the fault location. The samples of the voltage and current have to be synchronized from all ends of the transmission line. Such a method requires less than a cycle of voltage and current data and can provide an accurate estimate of the fault location before the opening of the breaker.

The results in this paper demonstrate that the algorithm developed in the next section does indeed satisfy the requirements above.

3. ALGORITHM DEVELOPMENT

The basis for the development of the fault analysis techniques is the selection of a proper model for the transmission line. Based on the length of the transmission line, the model can be one of the following:

- A lumped parameter, resistance-inductance model with the shunt capacitance neglected, for lines less than 50 miles long.
- A distributed parameter model with the shunt conductance neglected, for lines longer than 150 miles.

3.1 Short Line Algorithm

The short line algorithm therefore uses a model of the line as shown below in Figure 1.

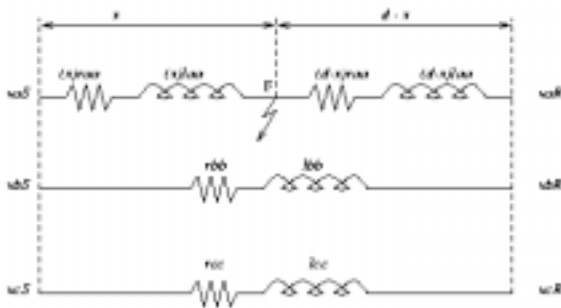


Figure 1: Model of a Short Transmission Line

The detailed derivation of the short line algorithm can be found in [4,5,6]. The basic idea is to write a time-domain, first-order differential equation that relates the 3 phase voltages and currents at the two ends of the line to the resistance and inductance of the line, at the fault point F . No assumptions are made about the line geometry. The self and mutual impedance of the three phases can be different from each other.

Writing the current as the difference between two consecutive samples divided by the sampling interval, as in Equation (1), approximates the continuous time derivative.

$$\frac{di}{dt} = \frac{i(k) - i(k-1)}{\Delta t} \quad (1)$$

Voltage and current samples are then acquired over one cycle at 60 Hz. At each sampling instant, the voltage at point F is written in terms of the voltage and current at the sending and receiving ends. The resulting set of equations is an over-determined set of equations, in which the only unknown is the distance to the fault from the sending end, x . The unknown fault location is estimated using a least square estimation method.

Let us assume that:

- There is no noise in the measurements
- The parameters of the line are known exactly
- There are no synchronization errors in the acquired samples

Under these assumptions, the accuracy of the fault location will be affected only by the sampling interval Δt . Small intervals will produce good approximations of the derivative, while larger intervals will produce approximations that lead to larger errors in the fault location estimation.

Since the algorithm uses less than a cycle worth of data, it is extremely fast, and produces good accuracy in locating the fault at sampling frequencies down to 4 kHz.

Extension of this algorithm to the case of mutually coupled and multi-terminal lines is possible if data can be acquired from all the line ends. One example of this can be found in [6].

3.2 Long Line Algorithm

The long line algorithm models the line with constant but distributed resistance, inductance and capacitance along the line length.



Figure 2: Unfaulted Long Transmission Line

R, L and C are measured in Ω , H and F per unit length of the line. The algorithm is developed for the single-phase line in Figure 2. The shunt conductance is neglected. The earlier development of the long line algorithm [4,5] considered the line to be lossless, by neglecting the series resistance. This parameter is included in the algorithm here. The voltage and current along the line are functions of both time and distance from the line ends. They are written as per the *Telegrapher's Equations* (2) and (3).

$$\frac{\partial v}{\partial x} + L \frac{\partial i}{\partial t} = -Ri \quad (2)$$

$$C \frac{\partial v}{\partial t} + \frac{\partial i}{\partial x} = 0 \quad (3)$$

The equations above can be solved using the method of characteristics, proposed by Collatz [8]. To solve the equations, the required boundary conditions are the voltage and current samples from the two ends of the line over a period of around one 60 Hz cycle. Cory and Ibe, [9], used this method to estimate the fault location on transmission lines. But their method is a single-ended method, depending on data from one end of the line. Moreover, the sampling frequency was required to be as high as 300 kHz, making it unsuitable for implementation in a field instrument.

Let us denote the voltage and current at the sending end by $v_S(0,t)$ and $i_S(0,t)$ respectively, and the voltage and current at the receiving end by $v_R(0,t)$ and $i_R(0,t)$ respectively. The fault location problem can then be stated as finding that point in the line where the voltage computed using the sending end data and the voltage computed using the receiving end data are the same, or closest to each other, when compared to other points in the transmission line.

The method of characteristics allows the development of a voltage profile along the line, starting from the data at the line ends. To be able to do this, the transmission line has to be divided into discrete segments, of a specific length, which is controlled by the sampling frequency.

$$\Delta x = \frac{\Delta t}{\sqrt{LC}} \quad (4)$$

$1/\sqrt{LC}$ is the surge velocity of the line and depends upon the inductance and capacitance per unit length of the line. Equation (4) indicates that the length of the discrete segment is directly proportional to the sampling interval. Our goal is to make these segments as short as possible, which means that the sampling interval should be as small as possible (high sampling rates). It is important to realize this because the method of characteristics will allow profile building only at the discrete points calculated using Equation (4).

Now, the voltage and current at any discrete point x_j at a time instant t_k can be written in terms of the voltage and

current at the previous discrete point x_{j-1} at two time instants, t_{k-1} and t_{k+1} respectively as in Equations (5) and (6).

$$v(x_j, t_k) = f[v(x_{j-1}, t_{k-1}), v(x_{j-1}, t_{k+1}), i(x_{j-1}, t_{k-1}), i(x_{j-1}, t_{k+1})] \quad (5)$$

$$i(x_j, t_k) = f[v(x_{j-1}, t_{k-1}), v(x_{j-1}, t_{k+1}), i(x_{j-1}, t_{k-1}), i(x_{j-1}, t_{k+1})] \quad (6)$$

According to equations (5) and (6), starting from the set of samples for the ends of the line, the voltage and current can be iteratively calculated for every discrete point in the line.

Once the number of discrete points have been calculated, the fault location proceeds as follows:

- **Locate the Approximate Fault Point:** At each discrete point, compute the voltage and current over a certain interval due to the sending end voltage and current. Repeat the procedure at the same point, but by using the voltage and current from the receiving end. Compute the square of the difference between the two voltages so computed. Then proceed to the next discrete point. If this voltage difference at each point is plotted, a figure similar to Figure 3 will be obtained. The point with the least error (difference) is picked as the approximate point.

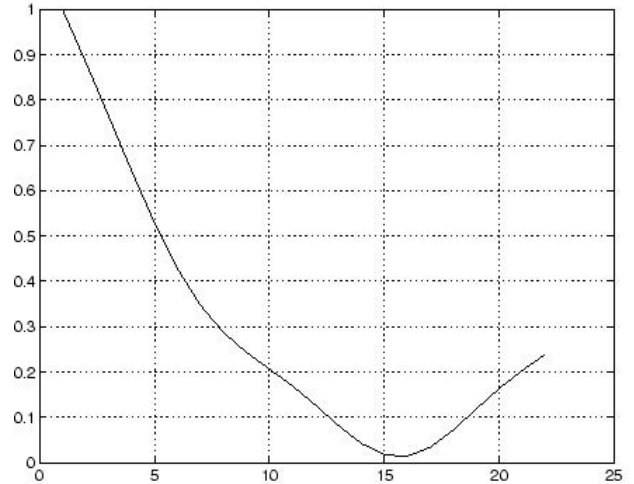


Figure 3: Location of the Approximate Fault Point

- **Refine the Fault Location:** Now the short line algorithm is applied on the line section that encloses the approximate fault point computed in the previous step.

At a sampling frequency of 20 kHz, the length of each discrete segment is 9.32 miles, assuming the velocity of the traveling wave to be the speed of light (3e8 m/sec). Therefore, the refinement of the fault location using the short line algorithm is necessary, to achieve any reasonable degree of accuracy in the fault location. A sampling frequency of 20 kHz is possible using specialized data acquisition equipment, but is not being currently used in standard power system applications.

3.3 Fault Detection and Classification

Fault detection and classification are based upon a lumped parameter transmission line model. The vector $\Delta I(t)$ is calculated based on the first-order differential equation relating the terminal voltages and currents to the parameters of the line. This quantity is the fault current flowing through the three phases. For fault detection, any deviation from zero of the quantity $\Delta I(t)$ is considered to be an indication of a fault on the transmission line.

For fault classification, the ground fault current is calculated from the samples of the individual phase fault current samples. The presence of fault current in any of the phases is indicative of a fault on that phase. To check if ground is involved in the fault, the ground fault current previously computed is checked.

The implementation details and test results can be found in [7].

4. SIMULATION AND TESTING

This section presents the results from testing the long line fault location algorithm on the data generated from simulating a model of a power system. The simulations were carried out in EMTP [10]. The power system is shown in Figure 4.

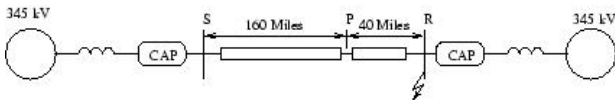


Figure 4: 200 Mile Transmission Line

Faults were introduced in the line at 20.0, 100.0 and 160.0 miles from the end S of the 345 kV line. Four types of faults (AG, BC, BCG and ABCG) at two different incidence angles (0° and 90°), at two different impedances (3Ω and 90Ω) were considered.

Also included in the testing were instrument transformers (CTs and CCVTs), to make the testing as realistic as possible. The models of the instrument transformers were developed earlier [11,12]. The following tables summarize the results from four different scenarios:

- **PC:** Data from **Primary**, Series Capacitors at line ends **included**
- **PN:** Data from **Primary**, Series Capacitors at line ends **excluded**
- **SC:** Data from **Secondary**, Series Capacitors at line ends **included**
- **SN:** Data from **Secondary**, Series Capacitors at line ends **excluded**

It is important to note that the sampling frequency used for the simulation was 4 kHz, which is within the capability of conventional power system data recording equipment. At this sampling frequency, the length of

each discrete segment is 46.6 miles. Before applying the fault location algorithm, the voltage and current data are up-sampled to 20 kHz, to artificially bring the length of each discrete segment to 9.32 miles.

In each cell of the table, the error in fault location is shown on the first line, with the estimated distance below it. The fault error percentage is calculated as

$$Error(\%) = \frac{|Computed\ Loc. - Actual\ Loc. |}{Line\ Length} \quad (7)$$

Actual Location	Fault Scenario			
	PC	PN	SC	SN
20.0	0.965 18.070	1.088 17.825	1.543 16.914	0.424 19.152
100.0	4.252 91.496	0.109 100.218	4.454 108.908	0.145 100.290
160.0	1.045 157.910	0.451 159.098	2.202 164.404	0.203 160.406

Table 1: Phase A to Ground Fault

Actual Location	Fault Scenario			
	PC	PN	SC	SN
20.0	0.898 18.204	0.697 18.606	1.185 17.63	0.330 20.659
100.0	1.556 96.889	0.513 98.973	0.842 98.316	0.318 99.364
160.0	0.768 161.536	0.831 161.663	1.036 157.928	0.845 161.690

Table 2: Phase B to C Fault

Actual Location	Fault Scenario			
	PC	PN	SC	SN
20.0	0.188 19.624	0.329 19.342	0.850 21.700	0.269 20.537
100.0	0.327 100.654	0.150 99.699	0.401 99.198	0.357 99.287
160.0	0.245 160.491	0.334 160.667	0.831 158.337	0.748 161.496

Table 3: Phase B to C to Ground Fault

Actual Location	Fault Scenario			
	PC	PN	SC	SN
20.0	0.225 19.551	0.250 19.500	0.943 21.866	0.187 20.374
100.0	0.714 101.428	0.214 100.428	0.502 101.004	0.059 99.883
160.0	0.200 160.400	0.319 160.638	1.082 157.836	0.677 161.354

Table 4: Phase A to B to C to Ground Fault

From the results, we see that the worst case error is seen for the AG fault at 100 miles from the sending end *S*, in Table 1. The worst case error in each table is highlighted. In all cases, the presence of series capacitors produces the largest error. Also, if data is acquired from the secondary of the instrument transformers, the error is larger for most cases, than when the data is acquired from the primary.

The tests conducted show that the error is not affected by the fault resistance or incidence angle of the fault. Therefore, for each fault location and scenario, we picked the largest of 4 possible errors (two incidence angles at two fault impedances) and have shown that number in each cell of the tables above.

The fault location and fault type do however affect the error produced by the algorithm. The method of characteristics can reconstruct the voltage and current profile at each discrete point accurately. However, when the reconstructed data is applied to the short line segment in the refinement phase of the fault location, there is a mismatch between the data and the model of the line that is being used for the refinement. This produces the variations in the errors for different fault types and locations.

The algorithm was then tested on a model of a power system in the Western Area Power Administration Grid. This system is shown in Figure 5. The line of interest is the 242.4 mile long transmission line between Mead and Westwing Substations at the 525 kV level. The system is quite complex, with mutual coupling between the 525 kV line and the 345 kV line between the Mead and Liberty substations. Series capacitor installations are present at each end of the line, along with line entry surge arresters and instrument transformers.

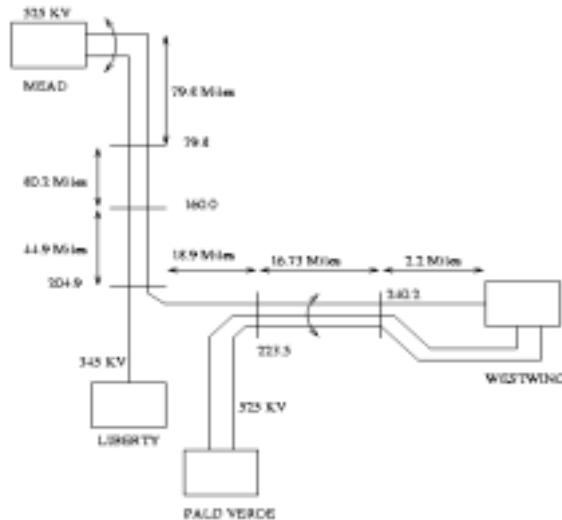


Figure 5: One Line Diagram of the Utility Power System

Data was acquired in this case from the Mead, Westwing and Liberty substations at the 525 kV and 345 kV levels. The existing fault location algorithm was extended to account for the extra data and the mutual coupling. The

algorithm did not account for the mutually coupled section between 223.5 miles and 240.2 miles (Palo Verde – Westwing 525 kV). This produced additional errors during the performance evaluation.

The performance of the multi-terminal algorithm followed the same general trends as the algorithm for the single line, with the maximum errors being seen for the cases with the capacitors included in the simulations.

5. FIELD IMPLEMENTATION ISSUES

Some of the issues associated with implementing such a fault locator as a viable field instrument are discussed in this section. A hardware setup that acquires data from the instrument transformers at the two ends of the line is shown in Figure 6.

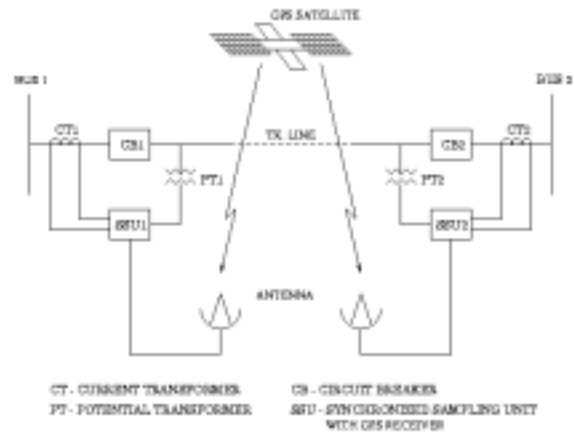


Figure 6: Synchronized Sampling Arrangement

The data acquisition units (SSU1 and SSU2) continuously sample the voltage and current signals from the instrument transformers and associate a time tag with each sample so acquired. The data from both ends is then transmitted to a computer that performs the fault location estimation.

The sampling units are also equipped with a GPS receiver that produces the time-tagging signal based on the inputs from the GPS satellites. While it is theoretically possible to achieve a time resolution of $\pm 0.5\mu\text{s}$ with the receivers, there are a number of factors that will introduce additional synchronization errors. These are:

- **Response of the voltage and current transformers:** The presence of these devices in the measurement path introduces a phase shift in the signals that are acquired. Since this phase shift cannot be measured, they cannot be compensated for while processing.
- **Phase shifts due to the electronic data acquisition equipment:** SSU1 and SSU2 are built using electronic filters and analog digital converters. The time it takes to process data through these components introduces variable delays in the sampled signals.

It is important to identify these sources of error and quantify, if possible, the maximum synchronization error that may be encountered.

Other issues to be considered are:

- **Sampling Frequency:** The sampling frequency determines the length of each discrete segment that the algorithm will see. We saw earlier in the paper that for a length of 9.32 miles, a sampling frequency as high as 20 kHz was needed. While this falls outside the range of existing power system data recorders, a special equipment can be built using DSP based data acquisition units from manufacturers like National Instruments. These units are capable of high sampling rates of 150 kHz or greater. The approach adopted in the paper is to use a 4 kHz rate, and then artificially up-sample the data to achieve a rate of 20 kHz. The errors due to this process will affect the accuracy of the fault location.
- **Measurement Noise:** The simulations in the paper are based on noise-less measurements. It is important to note that good anti-aliasing filters will be needed to remove the high frequency noise from the measurements.

6. CONCLUSIONS

This paper reviews some of the fault analysis techniques that have been developed at Texas A & M University in the past few years. The fault analysis function consists of fault detection, classification and location. The previous development in the area of fault location used a distributed parameter model of the transmission line, with the series resistance neglected from the model. In this paper, the algorithm is extended to account for the series losses in the line that helps in accurate voltage and current reconstruction along the line.

The method of characteristics is used to solve for the voltage and current at each discrete point in the line. This method starts from the ends of the line, and recursively builds the profile at each discrete point in the line.

Results from testing the algorithm show that it produces a good accuracy for most of the fault cases, although the errors do vary with the fault location and fault type. Testing was also carried out on a utility power system model.

Apart from improper modeling of the power system under study, GPS synchronization errors, noise in the measurements and the response of the instrument transformers are factors that affect the accuracy of the method. These have to be considered when designing a fault locator for use in the field.

ACKNOWLEDGMENT

Support for the fault location project was provided by Western Area Power Administration, under TEES contract 32525-50140.

REFERENCES

- [1] Working Group H-7 of the Relaying Channels Subcommittee of the IEEE Power Systems Relay-

- ing Committee (Chairman A. G. Phadke), "Synchronized Sampling and Phasor Measurements for Relaying and Control", *IEEE Transactions on Power Delivery*, Vol. 9, No. 1, pp. 442-452, January 1994.
- [2] J. Paserba, C. Amicella, R. Adapa, E. Dehdashti, "Assessment of Applications and Benefits of Phasor Measurement Technology in Power Systems", in *EPRI Wide Area Measurement Systems (WAMS) Workshop*, Lakewood, Colorado, April 1997.
- [3] K. E. Stahlkopf and M. R. Wilhelm, "Tighter Controls for Busier Systems", *IEEE Spectrum*, pp. 48-52, April 1997.
- [4] S.M. McKenna, D. Hamai, M. Kezunovic, A. Gopalakrishnan, Transmission Line Modeling Requirements for Digital Simulator Applications in Testing New Fault Location Algorithms, *Second International Conference on Digital Power System Simulators (ICDS '97)*, Montreal, Canada, May 1997.
- [5] M. Kezunovic, J. Mrkic and B. Perunicic, "An Accurate Fault Location Algorithm using Synchronized Sampling", *Electric Power Systems Research Journal*, Vol. 29, No. 3, May 1994.
- [6] B. Perunicic, A. Jakwani and M. Kezunovic, "An Accurate Fault Location on Mutually Coupled Transmission Lines using Synchronized Sampling", *Stockholm Power Technology Conference*, Stockholm, Sweden, June 1995.
- [7] M. Kezunovic and B. Perunicic, "Automated Transmission Line Fault Analysis using Synchronized Sampling at Two Ends", *IEEE Transactions on Power Systems*, Vol. 11, No. 1, pp. 441-447, February 1996.
- [8] L. Collatz, "The Numerical Treatment of Differential Equations", Springer-Verlag, 1966.
- [9] A. O. Ibe and B. J. Cory, "A Traveling Wave Fault Locator for Two- and Three-Terminal Networks", *IEEE Transactions on Power Delivery*, Vol. 1, No. 2, pp. 283-288, April 1986.
- [10] Electric Power Research Institute, "Electromagnetic Transients Program (EMTP)", *Version 2, Revised Rule Book*, Vol:1, Main Program, EPRI-EL-4541-CCMP, Palo Alto, California, March 1989.
- [11] M. Kezunovic, L. Kojovic, V. Skendzic, C. W. Fromen, D. R. Sevcik, S. R. Nilsson, "Digital Models of Coupling Capacitor Voltage Transformers for Protective Relay Transient Studies", *IEEE Transactions on Power Delivery*, Vol. 7, No. 4, October 1992, pp. 1927-1935.
- [12] M. Kezunovic, L. Kojovic, A. Abur, C. W. Fromen, D. R. Sevcik, F. Philips, "Experimental Evaluation of EMTP-Based Current Transformer Models for Protective Relay Transient Study", *IEEE Transactions on Power Delivery*, Vol. 9, No. 1, January 1994, pp 405-413.